2021-08-01

Study Of Weakly Bound Cluster Anions Using Self Interaction Corrected Density Functional Scheme

Peter Obinna Ufondu
University of Texas at El Paso

STUDY OF WEAKLY BOUND CLUSTER ANIONS

USING SELF INTERACTION CORRECTED

DENSITY FUNCTIONAL SCHEME

UFONDU PETER OBINNA

Master's Program in Computational Science

APPROVED:

Rajendra Zope, Ph.D., Chair

Tunna Baruah, Ph.D.

Natasha Sharma, Ph.D.

Stephen L. Crites, Jr., Ph.D.
Dean of the Graduate School

Dedication

To my family

STUDY OF WEAKLY BOUND CLUSTER ANIONS USING SELF INTERACTION CORRECTED DENSITY FUNCTIONAL SCHEME

by

UFONDU PETER OBINNA, M.Sc.

THESIS

Presented to the Faculty of the Graduate School of

The University of Texas at El Paso

in Partial Fulfillment

of the Requirements

for the Degree of

MASTER OF SCIENCE

Computational Science Program

THE UNIVERSITY OF TEXAS AT EL PASO

August 2021

Acknowledgements

I would like to thank all the people who contributed in some way to the work described in this thesis. First and foremost, I thank my academic supervisors Prof. Dr. Rajendra Zope and Prof. Dr. Tunna Baruah, for accepting me into the group. During my studies, they contributed to a rewarding graduate school experience by giving me intellectual freedom in my work, supporting my attendance at various conferences, engaging me in new ideas, and demanding a high quality of work in all my endeavors. Additionally, I would like to thank my committee member Dr. Natasha Sharma for her interest in my work. Every result described in this thesis was accomplished with the help and support of fellow lab-mates.

I would like to thank the various members of the electronic structure lab. with whom I had the opportunity to work and have not already mentioned: Dr. Luis Basurto, Dr. Yoh Yamamoto, Dr. Po-Hao Chang and Dr. Carlos Diaz. They provided a friendly and cooperative atmosphere at work and also useful feedback and insightful comments on my work.

I am grateful for the funding sources that allowed me to pursue my graduate school studies: The U.S Department of Energy, International Texas Public Education Grant, Betty Smith-Priest Endowed Scholarship, and Summer research Funding provided by graduate school.

My graduate experience benefited greatly from the courses I took, the opportunities I had under both in Physics department and Computational Science program to serve as either a research or teaching assistant, and the high-quality seminars that the department organized. Finally, I would like to acknowledge family and friends who supported me during my time here. First and foremost, I would like to thank my Mom, Vivian, Zois, Micheal, and Benedine for their constant love and support.

Abstract

The Kohn–Sham formulation of density functional theory (DFT) is a widely used quantum mechanical theory to study chemical and materials properties. The practical application of DFT requires an approximation to the exchange–correlation (XC) functional. These approximations suffer from self-interaction errors due to the incomplete cancellation of the self-Coulomb energy with the approximate self-exchange and correlation energy for one-electron densities. Systems with weakly-bound electrons impose great challenges to semi-local density functional approximations. We use recently developed local scaled self-interaction correction (LSIC) by Zope et al and the Perdew-Zunger SIC method using the Fermi-Löwdin orbitals to calculate the vertical detachment energies (VDEs) of ammonia cluster anions $(NH_3)_n^-, (n = 3 - 8)$. The results from the density plot difference show that these clusters bind the extra electron in dipole-bound states. The LSIC significantly reduces the errors in LDA and GGA calculations leading to better agreement with reference Coupled-Cluster with Single and Double and Perturbative Triple excitations CCSD(T) values. We also investigate the negative of highest occupied molecular orbital (HOMO) energy with DFA, FLOSIC, and LSIC to approximate the VDEs.

Table of Contents

List of Tables

List of Figures

List of Illustrations

Chapter 1: Introduction

It has long been recognized that many materials properties are governed by their electronic structure, yet only relatively recently has it become possible to apply density functional theory DFT to calculate these properties with predictive accuracy. DFT calculations are based on the Kohn-Sham ansatz which is computationally less expensive in solving self-consistent Schr¨odinger-like equations for each electron in the system [1, 2]. DFT is centered around the minimization of a total energy functional, which is exact except for the exchange and correlation term that is approximated [3]. Over the last decades, different density functional approximations DFAs for the exchange-correlation functional terms have been developed to improve the performance of DFT. However, several weaknesses of DFT have been noted and are attributed to the so-called self-interaction error (SIE) [4] which includes but not limited to the violation of Koopman's theorem [5] and an unphysical long-range behavior of the potential at the asymptotic region [6]. Systems of weakly bound electrons impose great challenges to DFAs calculation because the extra electron density is significantly diffused. For example, the removal of an electron from such a molecular framework has a long-range electron-molecule potential that decays as $1/r^2$ (charge-dipole) or faster. Although there have been previous studies examining the accuracy of DFT in estimating average experimental dipole moment and vertical detachment energies of solvated electrons.

A solvated electron is a free electron in a solution and the smallest possible anion [61]. It occurs widely although it is difficult to observe directly since their life is so short.[61] The presence of solvated electrons was first studied almost 40 years ago in water by pulse radiolysis measurements through its strong visible absorption band [62]. The ammonia solved electron is a well-known species for electrical charges in a liquid environment found in chemical and biological processes

[61]. Experimentally and theoretically, there has been increasing interest in the studies of solved ammoniated electrons. Davy observed, nearly two hundred years ago, that sodium was dissolved in liquid ammonia to produce a deep blue solution [63]. Later, Weyl et al [64] described this phenomenon in detail that it was attributed to the formation of ordinary chemical complexes for many years. Then, after having studied the properties of metal ammonia solutions, Kraus proposed that the blue color was due to solvated ammoniated electrons [65]. Haberland, Kondow et al [66] found that the minimum ammonia cluster anion size to bound an electron at high Rydberg states is n=35. H. W. Sarkas and coworkers [67] use photoelectron spectra to study linear cluster anions of ionized electrons, they conclude that the vertical detachment energy VDE values for the cluster of size n=41 to n=1100 increase smoothly from 0.55eV to 1.05eV with no abrupt changes and they are in embryonic forms that will mature to become condensed phase solvated electrons with increasing cluster size. Bence Baranyi et al [56] have researched smaller size ammonia cluster anion, using both the quantum chemical approach and the simulation of molecular dynamics to study linear ammonia clusters anion(n=3 to 8), claiming that the excess electron is bonded by a dipole bound and that the VDEs increases as the cluster size increases. Our group recently applied Fermi Lowdin self-interaction corrected density function theory FLOSIC [10, 11] to solvated electron water cluster anions (n=2 to 6) [59], We reported that the FLOSIC method predicts accurate localization of the excess electron, the vertical detachment energies of the electron and its eigenvalues are negative. In this thesis, we report the performance of using FLOSIC and local self-interaction corrected (LSIC) [58] methods to compute the VDEs and the localization of the excess electron for ammonia cluster anions (n=3 to 8). We used long-range Gaussian basis functions and three non-empirical functionals that are ranked according to Jacob's ladder, local spin density approximation (LSDA)[14], Perdew-Burke-Ernzerhof generalized

gradient approximation (PBE)[15, 16], and the strongly constrained and appropriately normed (SCAN) meta-GGA[17] functional for our study. Details about the FLOSIC and LSIC methods are provided in the next section.

Chapter 2: Theoretical Background

2.1.0: Density Functional Theory

2.1.1: Electronic Structure Theory.

From the non-relativistic quantum theory, the state of any given system is represented by a time-dependent vector in Hilbert space, $|\psi\rangle$. This vector obeys the famous Schrödinger equation

$$i\hbar\frac{\partial}{\partial t}|\psi(x,t)\rangle = \hat{\mathrm{H}}|\psi(x,t)\rangle. \qquad 2.10$$

wherein I denote the imaginary unit, $\hbar$ denotes the reduced Planck constant, $\frac{\partial}{\partial t}$ denotes the partial time derivation, and denotes the Hamiltonian operator. If the Hamiltonian is time-independent, the separation ansatz of

$$\hat{\mathrm{H}}|\psi(x,t)\rangle = e^{-i\frac{E_t}{\hbar}}|\psi(x)\rangle. \qquad 2.11$$

The so-called stationary Schrödinger equation gives:

$$\hat{\mathrm{H}}|\psi\rangle = E|\psi\rangle. \qquad 2.12$$

Herein, E denotes the total energy of the system in the stationary state $|\psi\rangle$ For a many-body system of N electrons and M nuclei interacting through a Coulomb potential, the Hamiltonian has the form [10]

$$\hat{\mathrm{H}} = -\frac{\hbar^2}{2m_e}\sum_i^N \Delta_i - \sum_{i,I}^{N,M}\frac{Z_I e^2}{4\pi\varepsilon_0|\vec{x}_i-\vec{X}_I|} + \frac{1}{2}\sum_{i\neq j}^{N}\frac{e^2}{4\pi\varepsilon_0|\vec{x}_i-\vec{x}_j|} - \sum_I^M\frac{\hbar^2}{2M_I}\Delta_I + \frac{1}{2}\sum_{I\neq J}^{N,M}\frac{Z_I Z_J e^2}{4\pi\varepsilon_0|\vec{X}_I-\vec{X}_J|}. \qquad 2.13$$

Herein, $\vec{x}_i$ denotes the position of an electron I with the mass m_e and the negative elemental charge −e, $\vec{X}_I$ denotes the position of a nucleus I with the mass M_I and the atomic number Z_I , Δ denotes the Laplace operator and ε_0 denotes the dielectric constant.

Neglecting spin for the moment, the stationary state $|\psi\rangle$. can be reformulated as the many-body wave function $\psi = \psi(\vec{x}_1, .., \vec{x}_N, \vec{X}_1, .., \vec{X}_M,)$. The mass of the nuclei is so enormous in comparison to the electron mass m_e that, the nuclei stand still from the electronic point of view, while the electrons themselves appear to be moving instantaneously from the perspective of the nuclei. This is called the Born-Oppenheimer or adiabatic approximation, and it leads to a separation of electron dynamics from nuclear dynamics, introducing the electronic Hamiltonian $\hat{\mathrm{H}}_e$. This electronic Hamiltonian is written as

$$\hat{\mathrm{H}}_e = \hat{T}_e + \hat{V}_{ext} + \hat{V}_{int} + \hat{V}_{II}. \tag{2.14}$$

Using Hartree atomic units ($\hbar = 4\pi\varepsilon_0 = m_e = \mathrm{e} = 1$) from now on, the electronic kinetic energy operator $\hat{T}_e$ is given as

$$\hat{T}_e = -\frac{1}{2}\sum_i^N \Delta_i, \tag{2.15}$$

the attractive Coulomb potential $\hat{V}_{ext}$ between the electrons and nuclei can be written as

$$\hat{V}_{ext} = -\sum_{i,I}^{N,M} \frac{Z_I}{\left|\vec{x}_i - \vec{X}_I\right|}, \tag{2.16}$$

and the repulsive Coulomb potential $\hat{V}_{int}$ between the electrons is formulated as

$$\hat{V}_{int} = \frac{1}{2}\sum_{i\neq j}^{N} \frac{1}{\left|\vec{x}_i - \vec{x}_j\right|}, \tag{2.17}$$

Finally, the repulsive Coulomb potential $\hat{V}_{II}$ between the nuclei is given as

$$\hat{V}_{II} = \frac{1}{2}\sum_{I\neq J}^{N,M} \frac{Z_I Z_J}{\left|\vec{X}_I - \vec{X}_J\right|}. \qquad 2.18$$

This last term is solely dependent on the positions of the nuclei, which are treated as parameters in the electronic Hamiltonian. For a given set of nuclear positions, $\hat{V}_{II}$ is but an approximation. Anyway, the matter of finding the most energetically favorable nuclear positions is only addressed after the electronic Hamiltonian has been solved. The solution to the stationary Schrödinger equation involving $\hat{\mathrm{H}}_e$ is a wave function of the form $\emptyset = \emptyset\,(\vec{x}_1, .., \vec{x}_N)$. The nuclear 3M degrees of freedom have been successfully eliminated in order to tackle a problem that depends only on the electron positions as basic variables. There are several approaches to solve the electronic stationary Schrödinger equation, but this thesis will concentrate on the method called density functional theory (DFT), including both the fundamental concepts and the practical proceedings. The rest of this section will be fully dedicated to DFT, starting with its basis, i.e. the theorems of Hohenberg and Kohn [14].

2.1.2: The Theorems of Hohenberg and Kohn.

Even with the simplifications made above, the number of spatial variables to be calculated in order to obtain the correct solution corresponding to the electronic Hamiltonian is still 3N. As no computer available today is powerful enough to make these calculations in a finite amount of time, it is logical that this obstacle was even more insurmountable back in the 1960s, when Pierre Hohenberg and Walter Kohn took on the challenge. Their first Hohenberg-Kohn theorem proclaims that, for any system of interacting particles moving in an external potential $\hat{V}_{ext}\,(\vec{x})$, said the potential is determined uniquely by the ground state particle density $n_0(\vec{x})$ of the system -

except for a constant [10, 14]. However, determining the external potential equals determining the Hamiltonian, which in turn determines all the wave functions of the ground state and the excited states. As the wave functions contain the complete information of the system, any property of the system can be interpreted as a function of this density $n_0\ (\vec{x})$ [10, 14].

This function depends on merely three spatial coordinates. Thus, the introduction of the ground state density as a new basic variable has led to the establishment of the term "density functional theory" for the Hohenberg-Kohn theorems and the ideas they spawned.

Unfortunately, as enlightening as this theorem is in this respect, it does not provide any actual solution to the stationary Schrödinger equation of electronic structure theory [10]. The second Hohenberg-Kohn theorem, however, states that a universal function for the total energy E[n], which depends on the particle density n($\vec{x}$), can be defined and that this function is valid for any external potential $\hat{V}_{ext}\ (\vec{x})$, [10, 14]. For any given $\hat{V}_{ext}\ (\vec{x})$, the global minimum value of this energy functional is the ground-state total energy of the system, and the density minimizing the functional equals the ground state particle density $n_0(\vec{x})$ [10, 14]. The universal energy functional of Hohenberg and Kohn E_{HK}[n] is written as

$$E_{HK}[n] = T_e[n] + E_{int}[n] + \int d^3x \hat{V}_{ext}\ (\vec{x}) n(\vec{x}) + \ \hat{E}_{II}. \qquad 2.19$$

Regarding our systems of N interacting electrons moving in a Coulomb potential generated by M nuclei, the total energy E_{HK}[n] is defined as

$$E_{HK}[n] = \langle \emptyset \rangle, \qquad 2.20$$

The electronic kinetic energy $T_e[n]$ is formulated as [10]

$$T_e[n] = \langle \emptyset \rangle, \qquad 2.21$$

the internal potential energy $E_{int}[n]$ is written as

$$E_{int}[n] = \langle \emptyset \rangle, \tag{2.22}$$

the external potential $\hat{V}_{ext}\ (\vec{x})$ is given as

$$\hat{V}_{ext}\ (\vec{x}) = -\sum_{i,I}^{N,M} \frac{Z_I}{\left|\vec{x}_i - \vec{X}_I\right|}, \tag{2.23}$$

and the electron density $n(\vec{x})$ is defined as

$$n(\vec{x}) = N \int dx^3 \vec{x}_N .. \int dx^3 x N |\emptyset(\vec{x}, \vec{x}_2, \dots, \vec{x}_{N)}|^2. \tag{2.24}$$

Again, it is important to mention that this total energy functional $E_{HK}[n]$ is only useful for finding the ground state total energy and the corresponding electron density, not for obtaining any properties of excited states. But even for the ground state, the second Hohenberg-Kohn theorem does not yield any explicit expressions for the kinetic energy functional $T_e[n]$ and the internal potential energy functional $E_{int}[n]$. This seems to make the search for a minimum value of $E_{HK}[n]$ by varying $n(\vec{x})$ impossible [10]. Fortunately, Walter Kohn and Lu Jeu Sham found an ansatz to make up for this deficit in the original Hohenberg-Kohn theorems in 1965, a year after the latter were published [13]. This Kohn-Sham ansatz will be the topic of the next section.

2.1.3: The Kohn-Sham Ansatz

Basically, this ansatz of Kohn and Sham consists of substituting the many-body system of the Hohenberg-Kohn theorems with an auxiliary system of non-interacting electrons [10, 12, 13,17, 18]. As such, the state of this auxiliary system is represented by a single-electron wave function $\psi(\vec{x})$ the so-called Kohn-Sham orbital, which is delocalized in nature [12]. The Kohn-Sham (KS) orbital is consequently determined by a single-electron auxiliary Hamiltonian $\hat{\mathrm{H}}_{aux}$, defined as

$$\hat{\mathrm{H}}_{aux} = -\frac{1}{2}\Delta + \hat{V}_{aux}(\vec{x}). \tag{2.25}$$

This Hamiltonian incorporates a yet undefined, mean-field potential term $\hat{V}_{aux}$. This auxiliary system is created in such a way as to possess a ground state electron density identical to the one of the original systems [10, 12]. Introducing spin, the wave function describing the state of the Kohn-Sham system $\psi(\vec{x})$ can be reformulated as $\psi^{\sigma}(\vec{x})$. In the ground state, the $N^{\sigma=\uparrow}$ majority spin electrons present in the system occupy the $N^{\sigma=\uparrow}$ majority spin orbitals $\psi_i^{\sigma=\uparrow}(\vec{x})$ corresponding to the $N^{\sigma=\uparrow}$ lowest energy eigenvalues $\varepsilon_i^{\sigma=\uparrow}$ for the majority spin, and the same is valid for the minority spin [10]. Accordingly, the ground state electron density $n(\vec{x})$ of the auxiliary system can be constructed from the orbitals as

$$n(\vec{x}) = \sum_{\sigma}\sum_{i}^{N^{\sigma}} |\psi_i^{\sigma=\uparrow}(\vec{x})|^2, \tag{2.26}$$

Furthermore, the total energy functional of Hohenberg and Kohn $E_{HK}[n]$, is rewritten as the Kohn-Sham functional $E_{ks}[n]$, which is of the form

$$E_{ks}[n] = T_{ks}[n] + \int d^3x \hat{V}_{ext}(\vec{x})n(\vec{x}) + E_H[n] + E_{xc}[n] \tag{2.27}$$

Herein, the kinetic energy of the non-interacting electrons $T_{ks}[n]$ is given as [10]

$$T_{ks}[n] = -\frac{1}{2}\sum_{\sigma}\sum_{i}^{N^{\sigma}} \langle\psi_i^{\sigma=\uparrow}(\vec{x})\rangle, \tag{2.28}$$

and the Hartree energy $E_H[n]$, a term constructed as an analogon of the classic Coulomb self-interaction energy of the density $n(\vec{x})$, is defined as

$$E_H[n] = \frac{1}{2}\int\int \frac{n(\vec{x})n(\overrightarrow{x'})}{|\vec{x} - \overrightarrow{x'}|} dx^3 dx'^3. \quad 2.29$$

Lastly, the exchange-correlation energy $E_{XC}[n]$ includes all the non-classical many-body effects needed in the functional to justify the equivalence of $E_H[n]$.

The mathematical expressions of $E_{XC}[n]$, the exchange-correlation energy can be expressed as

$$E_{XC}[n] = T_e[n] - T_{KS}[n] + E_{int}[n] - E_H[n]. \quad 2.30$$

Thus, it can be viewed as the difference between the kinetic and internal potential energies in the original many-body system of Hohenberg and Kohn and in the auxiliary non-interacting electron system of Kohn and Sham [10]. In order to find the global minimum value of the Kohn-Sham functional $E_{ks}[n]$, which means finding the correct ground state total energy and ground state electron density, the functional is varied with respect to the spin-dependent Kohn-Sham orbitals $\psi_i^\sigma(\vec{x})$. This leads to variational equations of the type given as

$$\frac{\delta E_{ks}[n]}{\delta \psi_i^{\sigma,*}(\vec{x})} = \frac{\delta T_{KS}[n]}{\delta \psi_i^{\sigma,*}(\vec{x})} + \left[\frac{\delta \int d^3x \hat{V}_{ext}(\vec{x}) n(\vec{x})}{\delta n^\sigma(\vec{x})} + \frac{\delta \hat{E}_H[n]}{\delta n^\sigma(\vec{x})} + \frac{\delta \hat{E}_{XC}[n]}{\delta n^\sigma(\vec{x})}\right] \frac{\delta n^\sigma(\vec{x})}{\delta \psi_i^{\sigma,*}(\vec{x})} = 0 \quad 2.31$$

Calculating the functional derivatives of 2.31 is written as,

$$\frac{\delta T_{KS}[n]}{\delta \psi_i^{\sigma,*}(\vec{x})} = -\frac{1}{2}\Delta\psi_i^\sigma(\vec{x}), \quad 2.32$$

$$\frac{\delta \int d^3x \hat{V}_{ext}(\vec{x}) n(\vec{x})}{\delta n^\sigma(\vec{x})} = \hat{V}_{ext}(\vec{x}), \quad 2.33$$

$$\frac{\delta \hat{E}_H[n]}{\delta n^\sigma(\vec{x})} = \frac{1}{2}\int d^3x' \frac{n(\vec{x}')}{|\vec{x}-\vec{x}'|} = \hat{V}_H(\vec{x})[n], \tag{2.34}$$

$$\frac{\delta \hat{E}_{XC}[n]}{\delta n^\sigma(\vec{x})} = V_{XC}^\sigma(\vec{x})[n], \tag{2.35}$$

and

$$\frac{\delta n^\sigma(\vec{x})}{\delta \psi_i^\sigma(\vec{x})} = \psi_i^\sigma(\vec{x}), \tag{2.36}$$

allows developing an effective Kohn-Sham Hamiltonian $\hat{H}_{KS}^\sigma$. This Hamiltonian acts on the spin-dependent orbitals $\psi_i^\sigma(\vec{x})$, yielding the so-called Kohn-Sham equations

$$(\hat{H}_{KS}^\sigma - \varepsilon_i^\sigma)\psi_i^\sigma(\vec{x}) = (-\frac{1}{2}\Delta + V_{KS}^\sigma(\vec{x}) - \varepsilon_i^\sigma)\,\psi_i^\sigma(\vec{x}) = 0 \tag{2.37}$$

$$V_{KS}^\sigma(\vec{x}) = \hat{V}_{ext}(\vec{x}) + \hat{V}_H(\vec{x})[n] + V_{XC}^\sigma(\vec{x})[n]. \tag{2.38}$$

Hence, the ground state density $n(\vec{x})$ is constructed from spin-dependent Kohn-Sham orbitals stemming from a Hamiltonian. The potential terms of this Hamiltonian are except for $\hat{V}_{ext}(\vec{x})$ all functionals of this very same density. The Kohn-Sham equations must be solved self-consistently for $n(\vec{x})$, $\hat{V}_H(\vec{x})[n]$ and $V_{XC}^\sigma(\vec{x})[n]$ [10].

In the following, a short look at three of the most common exchange-correlation approximations, LDA, GGA and Meta-GGA will be given. These are also the functionals employed for the calculations later in this thesis.

2.2.0: Functionals For Exchange and Correlation

2.2.1: Local Density Approximation LDA

The local spin density approximation LDA was developed by Kohn and Sham and it tells that, for a system where the electron density varies over space the exchange and correlation are primarily local phenomena. for a spin- unpolarized homogenous system the exchange energy is analytical as a function of the density in the LDA approximation

$$E_{xc}[n] = \int dx^3 \varepsilon_x^{LDA}(n(x)). \tag{2.39}$$

Where $\varepsilon_x^{LDA}(n(r))$ is the exchange energy density that depends on $n(x)$ and is defined as:

$$\varepsilon_x^{LDA}(n) = -\frac{3^{\frac{4}{3}}}{4\pi^{\frac{1}{3}}} n^{\frac{4}{3}} = -C_x^{LDA} n^{\frac{4}{3}} \tag{2.40}$$

For a spin-polarized homogeneous system the exchange energy is analytical as a function of the density in the LDA approximation:

$$E_{xc}\left[n^{\uparrow}, n^{\downarrow}\right] = \frac{1}{2}(E_{xc}\left[2n^{\uparrow}\right] + E_{xc}[2n^{\downarrow}]). \tag{2.41}$$

LDA gives close to correct exchange-correlation energy to systems that have a similar property to homogeneous systems like the close shell system, metal, and electron gas.

2.2.2: Generalized Gradient Approximation GGA.

The generalized gradient approximation exchange-correlation energy is a functional of, both the local spin densities and the local spin densities gradients known as the dimensionless enhance factor F(s)

$$s(x) = \frac{1}{\sqrt[3]{24\pi^2}} \frac{|\nabla n(x)|}{n(x)^{\frac{4}{3}}} \quad 2.42$$

there the GGA exchange-correlation define as:

$$E_x^{GGA}[n, \nabla n] = \int dx^3 \varepsilon_x^{LDA}(n(x)) F_x(s(x)) \quad 2.43$$

2.2.3: Strongly Constrained and Appropriately Normed SCAN.

The SCAN exchange-correlation energy is a functional of, both the local spin densities, the local spin gradients, and the kinetics energy density.

$$E_x[n] = \int d^3x \varepsilon_x^{unif}(n) F_x(s, \propto), \quad 2.44$$

Where

$$\varepsilon_x^{unif}(n) = -(\frac{3}{4\pi^2})(3\pi^2 n)^{\frac{1}{3}} \quad 2.45$$

And the exchange energy per particle of the uniform electron gas $F_x(s, \propto)$ is the exchange enhancement factor,

$$S = |\nabla n| / [2(3\pi^2)^{\frac{1}{3}} n^{\frac{4}{3}}] \quad 2.46$$

is the dimensionless density gradient.

Obviously, the three functionals possess their characteristic strengths and weaknesses, and their usefulness is heavily dependent on the system at hand. The development of new and better functionals remains one of the main challenges for advancing density functional theory within the Kohn-Sham ansatz. However, instead of creating an entirely original functional, it is often more practical to add a term to those already existing, in order to correct some of their more apparent shortcomings. Many of the corrections currently in use aim to eliminate the so-called self-interaction error (SIE) [10, 18, 19, 20]. The nature of this error and the different approaches to tackle it will be the topic of the following section.

2.3.0: Self Interaction Correction to Density Functional Theory

The self-interaction error SIE is responsible for several weaknesses DFT calculations often exhibit. For solids, the SIE has been identified as the source for the systematic underestimation of the semiconductor band gaps [18, 27, 28]. These gaps are calculated as differences of orbital energy eigenvalues - specifically, as the differences between the HOMO (highest occupied molecular orbital) and the LUMO (lowest unoccupied molecular orbital) energies [18, 27, 28]. In general, uncorrected DFT does not fulfill Koopman's theorem, which identifies the HOMO energy as the negative of the ionization potential and the LUMO energy as the negative of the electron affinity [10, 18, 28]. In Koopman's theorem, orbital relaxation processes are neglected [1, 32]. The disagreement with Koopman's theorem stems partly from the tendency of DFT to increase the orbital energies in a non-systematic way [30, 31].

Furthermore, in localized, electrically neutral systems, the effective Kohn-Sham potential $V_{KS}^{\sigma}(\vec{x})$ fails to reproduce the expected, asymptotically correct long-range behavior of $-1/r$ [22, 28, 29]. A third disadvantageous consequence of the SIE is that several experimentally stable negative

ions, e.g. ethylene carbonate, are calculated to possess positive HOMO energies by DFT, which does not give a good descriptor of the EA. In the following, the terms formally describing the SIE will be introduced. As a matter of fact, both the Hartree energy functional, expressed as [10, 12, 13]

$$E_H[n] = \frac{1}{2}\int\int d^3x d^3x' \frac{n(\vec{x})n(\overrightarrow{x'})}{|\vec{x} - \overrightarrow{x'}|} \qquad 2.47$$

and the exchange-correlation energy functional E_{XC}[n] contains terms that describe the unphysical interaction of an orbital with itself. In the former functional, the Coulomb self-repulsion of an electron is included, the latter incorporates the effect of an electron exchanging with and being correlated to itself. It is worth noting that the validity of these statements does not depend on the concrete exchange-correlation functional in use but is of a general nature. If the exact exchange-correlation functional $E_{XC,exact}$[n] were known, this would not pose a problem, as the self-interacting terms would perfectly compensate each other for each orbital. This phenomenon can be written as

$$E_{XC,exact}[n_i^\sigma, 0] + E_H[n_i^\sigma] = 0 \qquad 2.48$$

In this equation, n_i^σ represents the spin-dependent orbital electron density defined as $n_i^\sigma = |\psi_i^{\sigma=\uparrow}(\vec{x})|^2$. However, as only approximate exchange-correlation functionals $E_{XC,appr}$[n] are applied in practice, this equation is sadly not fulfilled for any of the orbitals, resulting in the presence of the self-interaction error energy E_{SIE} in the functional. It is defined as

$$\sum_{\sigma}\sum_{i}^{N^{\sigma}} E_{XC,appr}[n_i^{\sigma}, 0] + E_H[n_i^{\sigma}] = E_{SIE}[n_1, n_2, \dots.]. \quad 2.49$$

Eliminating E_{SIE} is thus the aim of self-interaction corrections (SIC) to density functional theory. The SIC methods, proposed by Perdew and Zunger and the approach used by Mark Pederson et al will be presented in the following subsections [20, 22, 29].

2.3.1: Perdew-Zunger Self Interaction Correction(PZSIC)

The problem of self-interaction error which occur in density functional theory such as Rydberg state missing, mis-ordering of states of some systems, incorrect description of stretch bonds, problems with unstable anions due to the fact that the sum of the Hartree interaction energy and the approximated exchange correlation energy does not properly vanish for all one-electron system. This led to the introduction of self-interaction correction SIC proposed by Perdew and Zunger.

In their approach, they introduce orbital -dependent corrections to the exchange-correlation energy functional:

$$E_{xc}^{pZ}\left[n^{\uparrow}, n^{\downarrow}\right] = E_{xc}\left[n^{\uparrow}, n^{\downarrow}\right] - \sum_{\sigma}\sum_{i}^{N_{\sigma}}\{U[n_{i\sigma}] + E_{xc}[n_{i\sigma}, 0]\}. \quad 2.50$$

For the correct exchange-correlation functional, the correction should vanish. Where $n_{i\sigma}$ is the number of occupied orbitals of spin σ; is the orbital density for the KS orbital $\varphi_{i\sigma}$

$$n_{i\sigma} = |\varphi_{i\sigma}|^2 \quad 2.51$$

the total energy of an N-electron system is

$$E^{pz} = E^{DFT}[n] + \sum_{i} U^{SIC}[n_i] \quad 2.52$$

The Schrodinger-like equations like that of the Kohn-sham equations for N-electron system are got by varying the E^{pz} with respect to spin-orbital φ_i^{σ}

$$\{H_{0\sigma} + V_{i\sigma}^{SIC}\}\varphi_{i\sigma} = \sum_j^N \lambda_{ij}^{\sigma}\varphi_{j\sigma} \quad 2.53$$

The PZ-SIC leads to an energy expression that is not unitarily invariant. The PZ-SIC scheme is effective with small systems such as atoms using Kohn-Sham orbitals but for larger systems use of KS orbitals can lead to a size extensivity problem which means that the SI corrections for the total system are not equal to the sum of the corrections for the parts. The size-extensivity problem can be avoided by employing localized orbitals. Pederson et al. have shown that the localized orbitals need to satisfy the localization equations to ensure that the SI corrected total energy is minimized. The localization equations are:

$$\langle \varphi_{j\sigma} \rangle = 0 \quad 2.54$$

However, solving the localization equations on top of the KS equations makes it computationally expensive to apply SI corrections and therefore SIC calculations have been limited to small molecules only.

2.3.2: Fermi Löwdin Self-Interaction Correction (FLOSIC)

Within the FLOSIC approach, the necessity of solving the computationally demanding localization equations vanishes. Using the FLOSIC approach the localized orbitals are constructed based on the fermi orbitals. For a spin system of N number of electrons, the starting point is to have the Kohn-Sham occupied orbitals $\varphi_{i\sigma}$ transformed into Fermi orbitals $F_{i\sigma}$ which is defined by [40,41,42,43,44]

$$F_{i\sigma} = \frac{\sum_i^{N\sigma} \varphi_{i\sigma}^* a_{i\sigma}\varphi_{i\sigma}(\vec{x})}{\sqrt{\sum_i^{N\sigma} |a_{i\sigma}\varphi_{i\sigma}|^2}} = \sum_i^{N\sigma} F_{ij}\varphi_{i\sigma}(\vec{x}) \quad 2.55$$

In the above equation, $a_{i\sigma}$is the Fermi orbital descriptor FOD that describes the classical electronic position. Furthermore, the FODS is the variational parameters for minimizing the orbital dependent part of the energy and the F_{ij} is the fermi orbital transformation matrix.

The density of the Fermi orbitals is equal to the spin density of the KS-orbital and it is normalized since the Kohn-Sham orbital is orthonormal.

$$\left|F_j^{\sigma}(\vec{a}_j)\right|^2 = n^{\sigma}(\vec{a}_j) \tag{2.56}$$

The Lowdin's method of symmetric orthonormalization applied to the FOs, the orbitals are written in Hilbert space

$$\varphi_{i\sigma} = |\varphi_i\rangle \tag{2.57}$$

The overlap matrix S_{ij} is the representation of the Fermi orbitals$|F_i\rangle$

$$S_{ij} = \langle F_j\rangle \tag{2.58}$$

By Diagonalizing the overlap matrix of the Fermi orbitals which is solving the eigenvalues equations, the eigenvalues $Q_{\propto}$ is the measure of the captured charge by each intermediate Lowdin orbitals (ILOs). For the l-th, LO associated with it are derived by

$$\sum_i S_{ij}T_{lj} = Q_l T_{li} \tag{2.59}$$

where

$$T_l = \sum_j T_{lj}|F_j\rangle \tag{2.60}$$

and

$$|\emptyset_m\rangle = \sum_i \frac{i}{\sqrt{Q_l}} T_{lm}|T_l\rangle \tag{2.61}$$

The transformation of the FOs into FLOs is written as:

$$|\emptyset_m\rangle = \sum_{i,j,l} \frac{i}{\sqrt{Q_l}} T_{lm} T_{lj} |F_l\rangle \qquad 2.62$$

The total minimum energy associated with the set of FODs is derived by varying the initial FODs positions until the Hellmann-Feynman force $\vec{F}_{FOD}$ is at it minimum 10^{-3}.

The Hellmann-Feynman force is given by:

$$\vec{F}_{FOD} = \sum_{\sigma} \sum_{j}^{N^{\sigma}} -\nabla_{\sigma a_j} E_{PZ}[n_1, n_2 \ldots]. \qquad 2.63$$

The SIC total minimum energy is written as:

$$\left(\hat{H}_{PZ}^{m,\sigma} - \varepsilon_m^{\sigma}\right)\emptyset_m^{\sigma}(\vec{r}) = \left(-\frac{1}{2}\Delta + V_{PZ}^{m,\sigma}(\vec{r}) - \varepsilon_m^{\sigma}\right)\emptyset_m^{\sigma}(\vec{r}) = 0 \qquad 2.64$$

However, the self-consistent solution to the total minimum energy must be determined for each set of FODs which is calculated during the optimization process.

This chapter ends with the derivation of the local scaled self-interaction correction theory and then, the next chapter gives details about the computational application to ammonia cluster anions.

2.3.3: Local Scaled Self-Interaction Correction (LSIC)

LSIC method applies PZSIC correction locally in space and uses the iso-orbital indicator to assess the size of SIC correction as follows [58]:

$$z_{\sigma}(\vec{x}) = \tau_{\sigma}^{w}(\vec{x})/\tau_{\sigma}(\vec{x}) \qquad 2.65$$

Here, $\tau_{\sigma}^{w}(\vec{x})$ is the kinetic energy density of von Weiszcker and $\tau_{\sigma}(\vec{x})$ is the kinetic energy density of Kohn-Sham.

$$E_{XC}^{LSIC-DFA} = E_{XC}^{DFA}[n_i] + \sum_i \{U^{LSIC}[n_{i,\sigma}(\vec{x})] + \sum_i \varepsilon_{XC}^{LSIC}[n_{i,\sigma}(\vec{x}), 0]\} \qquad 2.66$$

The total LSIC-LSDA energies (Eq. (2.57)) were calculated using the corresponding PZSIC-LSDA self-consistent density and optimized local orbitals [58]. where

$$U^{LSIC}\left[n_{i,\sigma}(\vec{x})\right] = \frac{1}{2}\int d\vec{x}[z_\sigma(\vec{x})]n_{i,\sigma}(\vec{x})\int d\vec{x}'\,\frac{n_{i,\sigma}(\vec{x})}{\left|\vec{x}-\vec{x'}\right|} \qquad 2.67$$

and

$$E_{XC}^{LSIC}[n_{i,\sigma}(\overline{x}),0] = \int d\overline{x}[z_\sigma(\overline{x})]n_{i,\sigma}(\overline{x})E_{XC}^{DFA}[n_{i,\sigma},\overline{x}]. \qquad 2.68$$

Chapter 3: Methodology

The calculations on ammonia cluster anion $(NH_3)_n^-, (n = 3 - 8)$ are done using the LSIC approach implemented in the FLOSIC code 0.2[57, 58] on the UTEP version of the Naval Research Laboratory Molecular Orbital Library (NRLMOL)[39]. This is massive parallel code for electronic structure calculations and it uses Gaussian basis functions [40-46] and variational integration mesh to perform numerically precise calculations on atoms, molecules, and clusters. For these calculations, the structures of molecules are taken from Baranyi et al [46] and there is no further optimization of geometry for comparison purposes.

Table 3.1: Optimized Nrlmol basis sets with extra long-range extra Gaussian.

Atom	Exponents	s,p,d
H	0.77840802D+02 0.11534417D+02 0.26138581D+01	6,6,3
	0.73216633D+00 0.22838190D+00 0.74506970D-01	
Extra	0.2483565667D-01 0.8278552200D-02	
N	0.7806165340D+04 0.1785836240D+04 0.5074092930D+03	7,6,5
	0.5175062370D+05 0.1658509660D+03 0.5984476610D+02	
	0.2313469890D+02 0.9418458910D+01 0.3941794820D+01	
	0.1622742640D+01 0.6526657200D+00 0.2543715500D+00	
	0.9411174000D-01	
Extra	0.1568529000D-01 0.2614215000D-02	

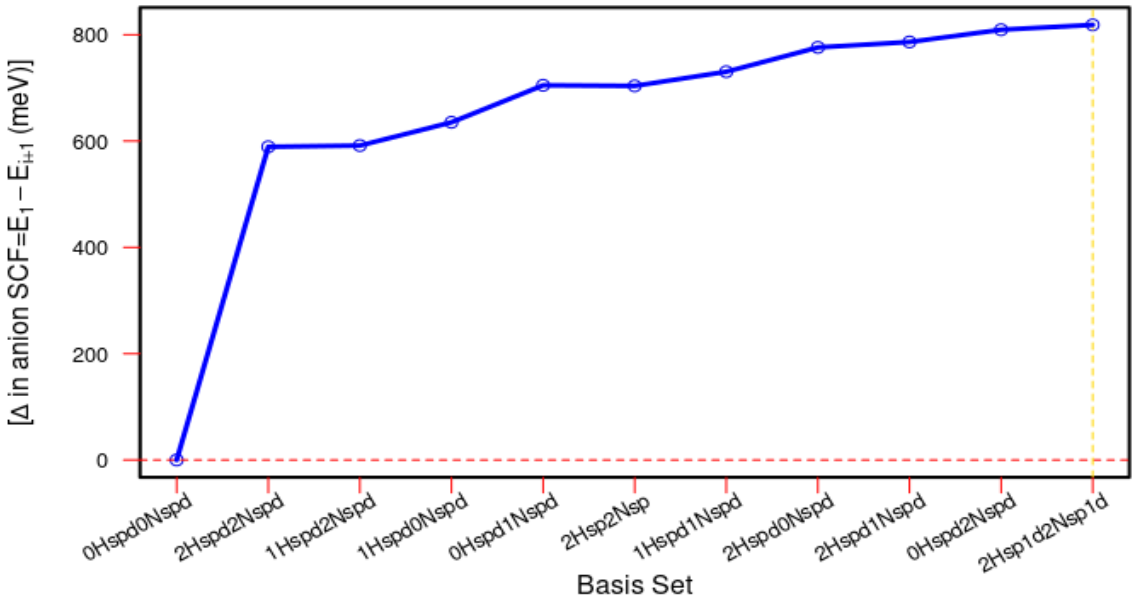

Illustration 3.1: Basis set convergence for linear chain ammonia cluster anions.

The yellow vertical line indicates the converged basis set used for this calculation. The extra long-range Gaussians were chosen such that one-third (1/3) of the (N) the exponent for hydrogen and one-ninth (1/9) of the $(N)^{th}$ the exponent for nitrogen is the $(N+1)^{th}$ Gaussian exponent respectively. These extra long-range Gaussians exponents are optimized at the SCAN level using the trimer anion for the calculations. In addition, preliminary calculations performed with default Gaussian basis sets, systematically yield a very large negative vertical detachment energy. A noticeable improvement is achieved by using extra long-range Gaussians shown in Illustration 3.1. However, in order to achieve basis sets convergence of the systems, the basis sets were designed by adding extra contracted Gaussian two sp and one d of diffuse functions on the nitrogen and two spd3 on the hydrogen, each set share the same extra long-range Gaussians exponent as can be seen from Illustration 3.1 to yield a negligible change in the total energy.

The rest of the calculations were done with the largest basis set indicated with a vertical yellow line as shown in Illustration 3.1. A self-consistent FLOSIC calculation is performed using the PW91-LDA, PBE-GGA, and SCAN. Regarding the LSIC calculations, PW91-LDA, PBE-GGA calculations are performed and the molecular geometry and the wave function were adopted from the previous FLOSIC calculations because of efficiency reasons. The classical electronic positions FODs were optimized to obtain structures with forces below 10^{-3} Ha/Bohr. For all molecules and using the three functionals, further calculations (anion) were performed with one electron added to the optimized neutral molecule without relaxing the molecular geometry. This was done in order to obtain the vertical detachment energy (E_{VDE}) values, which are defined as differences between the total energies of the neutral molecule and the anion at the anion geometry.

$$E_{VDE} = E_N - E_{N+1} \qquad 3.1$$

Herein, $E_N$and E_{N+1} represents the total energy of the Neutral molecule and anion. The values of the excess electron binding energies for $(NH_3)_n^-, (n = 3 - 8)$ as well as the dipole moment for the neutral molecules are obtained and compared with the already published literature.

To visualize the electronic geometries of the molecules, figures were created using the program Jmol [60]. In these figures, the structures were constructed using the atoms of the respective molecules, applying the optimized molecular FODs which were obtained at the FLOSIC calculations. Moreover, the FODs were assumed to occupy the positions of the electron orbitals, which were taken from the converged FLOSIC GGA calculation. The FODs were represented by red is the extra FOD is located at a distance away from the cluster. The FOs of each spin channel was connected to yield an approximate tetrahedron around the nitrogen and hydrogen atoms.

Chapter 4: Results and Conclusion

4.1: Linear Chain Ammonia Cluster Anions

We studied linear chain ammonia cluster anions $(NH_3)_n^-, (n = 3 - 8)$ from trimer to octamer having twisted lines bound by successive hydrogen bonds.

In Fig 4.1.1 we plot the deviation which is the difference between the computed values and the corresponding CCSD(T) values of the VDEs versus the size of the linear chain ammonia cluster using three functional for DFA and FLOSIC and two functional for LSIC and their corresponding highest occupied molecular orbital energy.

Table 4.1.1: Computed deviation for the vertical detachment energies, highest occupied molecular orbital energy, mean absolute deviation (MAE) and mean error (ME) of linear chain ammonia cluster anions.

ISOMER	DFA			FLOSIC			LSIC		MP2	FLOSIC HOMO			LSIC HOMO	
	LDA	PBE	SCAN	LDA	PBE	SCAN	LDA	PBE	MP2	LDA	PBE	SCAN	LDA	PBE
Trimer	190.710	174.700	62.860	73.310	51.540	15.610	-15.866	26.560	-18.500	42.180	14.740	17.620	17.089	-5.830
Tetramer	214.440	192.140	58.090	88.470	55.370	29.280	-14.826	32.000	-24.600	49.550	10.270	17.930	12.889	-16.200
Pentamer	230.050	202.220	61.190	93.440	63.500	32.010	-23.621	35.630	-29.500	49.110	9.350	23.960	8.751	-25.130
Hexamer	245.010	215.160	61.560	103.370	68.870	35.630	-18.666	28.300	-32.600	53.200	6.880	18.840	5.477	-31.120
Heptamer	253.500	221.010	63.780	94.320	50.390	-25.340	-54.954	37.040	-36.000	53.060	9.730	17.330	3.269	-36.220
Octamer	265.640	224.960	106.650	118.760	87.630	42.380	-33.270	27.540	-37.000	59.210	7.400	20.630	6.583	-36.470
MAE	233.225	205.032	69.022	95.278	62.883	30.042	26.867	31.178	29.700	51.052	9.728	19.385	9.010	25.162
ME	233.225	205.032	69.022	95.278	62.883	21.595	-26.867	31.178	-29.700	51.052	9.728	19.385	9.010	-25.162

A number of observations follow from Table 4.1.1. First, the results for the uncorrected LSDA, PBE, and SCAN calculations exhibit very similar trends for the cluster. All three methods generally overestimate the VDEs. Overall, the SCAN results agree somewhat better with the reference value than LSDA and PBE. Typical deviations for LSDA and PBE lie between 175 meV and 300 meV, while the deviation for each isomer for SCAN is mostly less than 70meV, except for octamer with a deviation of 106 meV. FLOSIC generally reduces the deviations of the computed VDEs for the ammonia cluster anions for all three functional, in nearly all cases bringing them closer to the reference values. However, the deviations are reduced to less than 100 meV for FLOSIC-LSDA and less than 88 meV and 43 meV for FLOSIC-PBE and FLO-SCAN. Results for

FLOSIC-LSDA, FLOSIC-PBE, and FLOSIC-SCAN also show similar overall trends against the size of the cluster, except for the FLO-SCAN heptamer cluster with deviation in the opposite direction.

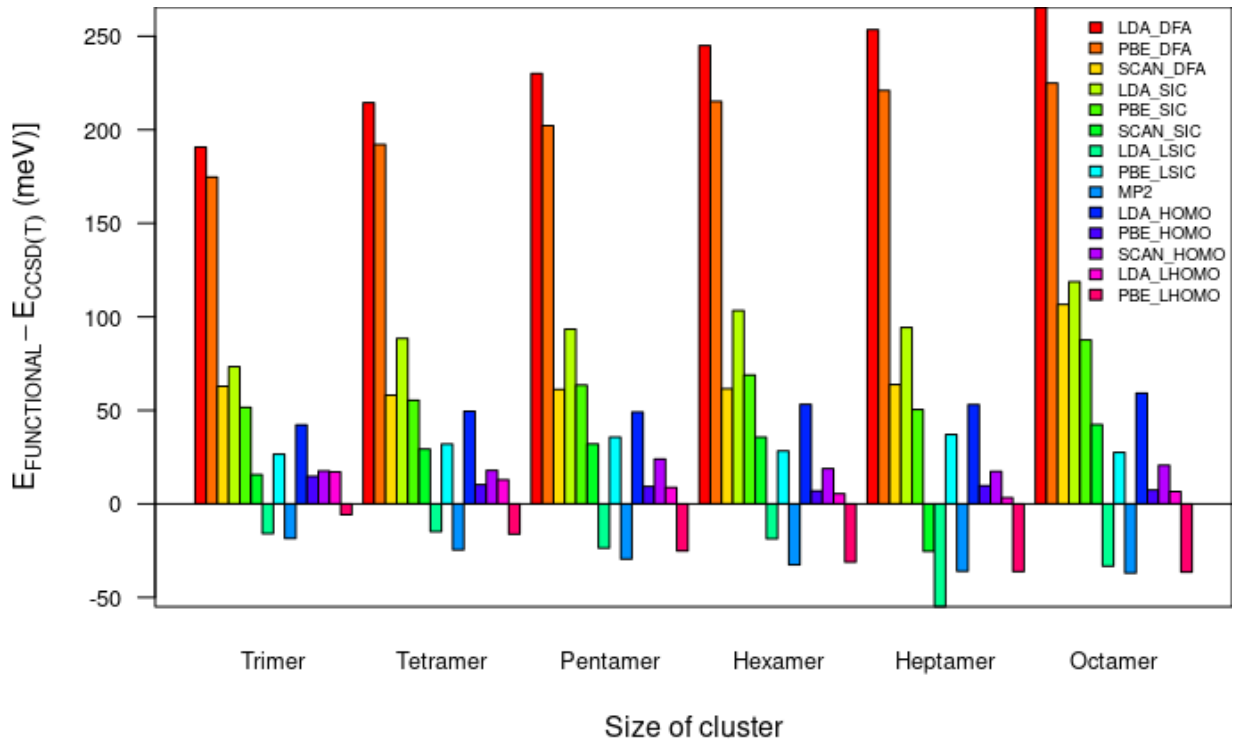

Illustration 4.1.1: Deviation of the Vertical detachment energies and highest occupied molecular orbital energy of linear chain ammonia cluster.

LSIC calculations reduce the deviation more significantly for both LSIC-LSDA and LSIC-PBE.

LSIC-LSDA and LSIC-PBE both have the deviation in the opposite direction for all clusters. For LSIC-LSDA, the deviation relative to reference values for both LSIC-LSDA and LSIC-PBE lies between 55meV to -14 meV and 26 meV to 38 meV respectively. The LSIC-LSDA results are in better agreement with the reference CCSD(T) values than that of MP2 results except for heptamer isomer whose deviation for LSIC-LSDA and MP2 are -55meV and -36meV respectively. DFA, over-bind the extra electron and thereby raise the DFA HOMO energies to be positive which

implies that the extra electron is not bound [5] but is artificially bound due to the infinite basis set limit used for these calculations. To further investigate the binding of the extra electron, we show in Table 4.1.1 the deviation of the FLOSIC and LSIC calculated orbital energy of the highest occupied orbital (HOMO) from the reference CCSD(T)[56] VDEs for linear chain ammonia cluster anions. The self-interaction correction SIC methods HOMO energies are negative, shows the importance of applying SIC to a system with diffused extra electrons. In Illustration 4.1.1, FLOSIC-PBE results agree with the reference values [56] vertical detachment energies pretty well, on average overestimating the reference values by only about 10 meV. The FLOSIC LSDA and SCAN HOMO energies, by contrast, overestimate the vertical detachment energies by roughly 51 meV and 19 meV on average. Interestingly, LSIC reduces the HOMO energies deviation for all clusters on an average of 42 meV and 34 meV from FLOSIC-LSDA to LSIC-LSDA and FLOSIC-PBE to LSIC-PBE. This supports the conclusion that the poor performance of the DFAs methods for the weakly bound anions to over-binding the extra electron is due to SIE.

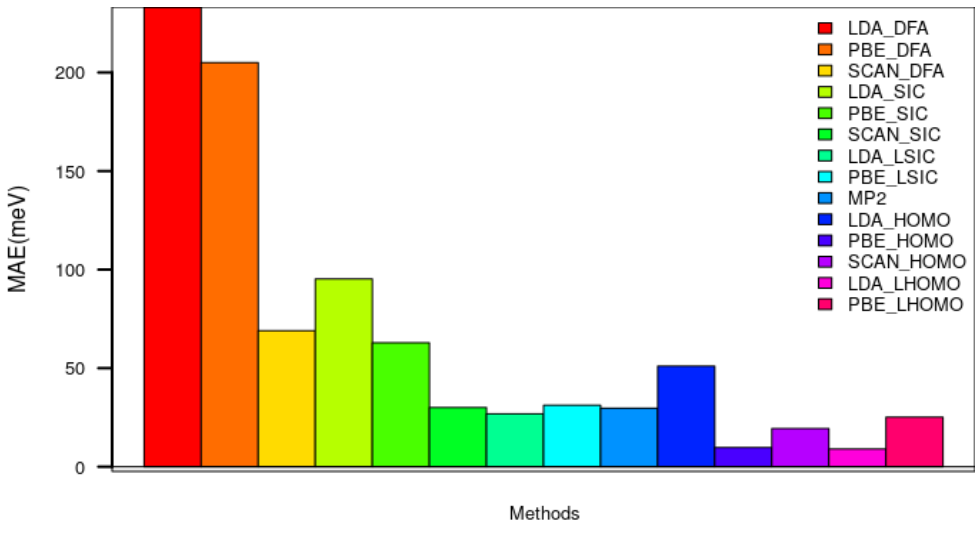

Illustration 4.1.2: Calculated Mean absolute deviation (MAE) of the Vertical detachment energies and highest occupied molecular orbital energy of linear chain ammonia cluster anions.

In Illustration 4.1.2 we show the mean error (ME) and mean absolute error (MAE) i.e mean sign and unsigned error compared to CCSD(T) values for the linear chain ammonia cluster anions. Comparison of the ME and MAE values are the same for the DFAs calculations, this implies that these DFAs generally overestimate the reference values. Results from our DFAs LSDA, PBE, and SCAN calculations are similar, respectively, with ME and MAE of 223 meV, 205 meV, and 69 meV. FLOSIC clearly improves the VDEs of LSDA and PBE, reducing the ME and MAE to 96 meV and 62 meV for FLO-LSDA and FLO-PBE. For SCAN, however, while FLO-SIC reduces the ME and MAE to 21.5 meV and 30 meV, the MAE changes because SCAN underestimates the VDE for heptamer. Applying the LSIC methods, the VDEs ME and MAE are -26.8meV, 31.2 meV, and 26.8 meV, 31.2 meV, for LSDA and PBE respectively. LSIC LSDA and PBE have opposite signs for mean error. This means that the LSDA and PBE underestimate and overestimate the reference CCSD(T) VDEs5values. The MAE for the HOMO energies is seen in fig 4.1.2 to be improved from 51 meV to 9 meV for FLOSIC LSDA and LSIC-LSDA, which is a better estimate of the VDEs. These results indicate that LSIC LSDA gives the best improvement in calculated VDEs for dipole bound anions using total energy or HOMO energy with LSDA functional.

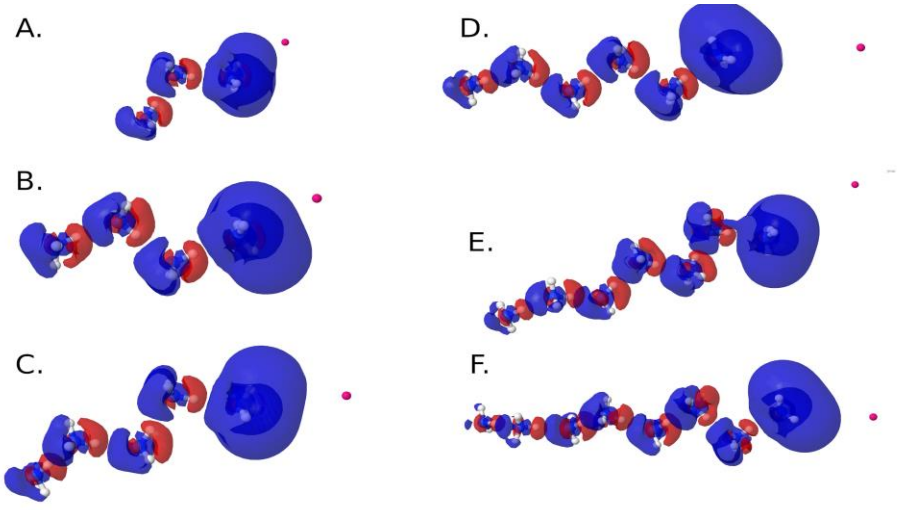

Figure 4.1.1: Ammonia cluster anion density difference with isovalue of 0.0000156.

The linear chain molecule is shown in FIG 4.1.1. This plot is from optimized FODs from the FLOSIC GGA calculations. The blue and red loop is positive and negative difference of the density. From this plot, we see that the blue loop is envelope over one molecule of the ammonia cluster anion that shows that the density of the extra electron is significantly diffused and the density of the charges are seen decreasingly distributed along the chain. The resulting isosurfaces surround more than 60 percent of the total density from trimer to octamer at an isovalue of 0.0000156. The excess electron localizes in a diffuse dipole bound state at the three dangling hydrogen atoms of the hydrogen-bond acceptor end of the chains.

Lastly, this interaction between the excess electron and the chain ammonia cluster is characterized to be DIPOLE BOUND. Such a system is very important and should be calculated with a very diffused gaussian basis set. From Figure 4.1.1. (A) Trimer, (B) Tetramer, (C) Pentamer, (D) Hexamer, (E) Heptamer and (F). Octamer. The blue and red loop is the density difference between the anion and neutral, the neutral and anion respectively. The magenta spheres represent the position extra FOD.

4.2: Branch Chain Ammonia Cluster Anions

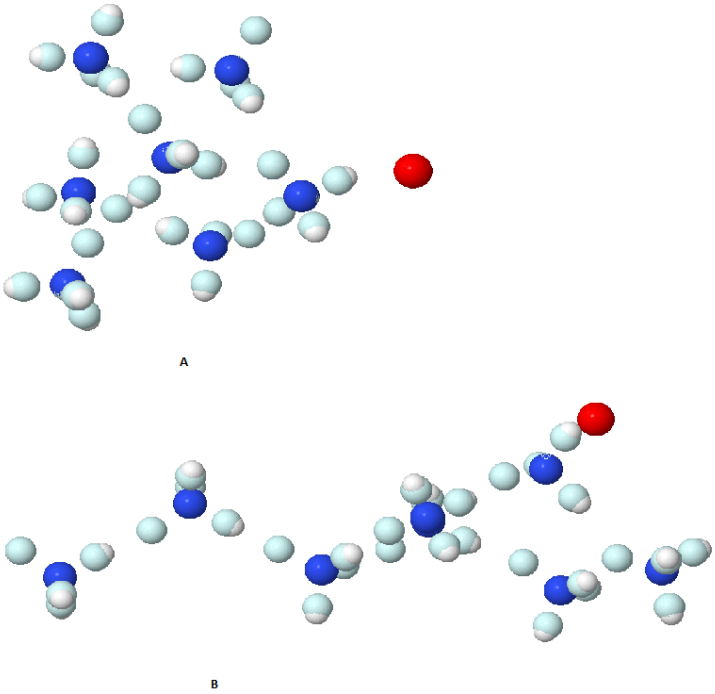

Figure 4.2.1: Branched chain ammonia cluster anion (A) Heptamer FODs configuration, (B)Octamer FODs configuration. The red sphere is the FOD for the extra anion.

We computed the relative energies and looked at deviation of vertical detachment energy for two clusters with branched hydrogen bond isomers each for heptamer and octamer clusters using FLOSIC and LSIC with LSDA and PBE functionals. The geometry for branched octamer structure on the right can be seen to have a linear trimer cluster having it end hydrogens bonded to dimer and trimer unlike the heptamer whose bounding form a spherical.

It is seen from Table 4.2 that relative energies for heptamer cluster is higher for the branch isomer and for octamer cluster it is lower for the linear isomer with both methods using the two functionals. For FLOSIC and LSIC with LSDA and PBE, the relative energy is lower for the branched heptamer by (68.73meV, 67.60meV and 80.89meV, 90.35meV) while relative energies are higher for branched octamer by (127.54meV, 79.83meV and 87.48meV, 96.79meV) respectively.

Table 4.2.1: Computed relative vertical detachment energy, change in the vertical detachment energy and highest occupied molecular orbital energy, mean absolute deviation (MAE) and mean error (ME) of branched chain ammonia cluster anions.

ISOMER	FLOSIC						LSIC							
	LDA			PBE			LDA			PBE			MP2	
	VDE	ΔVDE	$\Delta HOMO$	VDE	ΔVDE	$\Delta HOMO$	VDE	ΔVDE	$\Delta HOMO$	VDE	ΔVDE	$\Delta HOMO$	VDE	ΔVDE
Heptamer B	172.59	102.23	57.78	129.8	59.44	9.59	11.16	-59.2	24.59	93.69	23.33	-4.31	35.19	-35.16
Octamer B	410.3	159.77	89.83	331.45	80.92	2.56	218.21	-32.32	0.09	288.33	37.8	-70.78	193.34	-57.2
MAE		131.0	73.8		70.1	6.0		45.7	12.3		30.5	37.5		46.1
ME		131.0	73.8		70.1	6.0		-45.7	12.3		30.5	-37.5		-46.1

From table 4.2.1 the VDE computed by both change is total energy and absolute of the HOMO energy by FLOSIC LSDA and PBE calculations have a ME and MAE of 131 meV , 73.805 meV and 70.18 meV, 6.075 meV are seen to have same signs for the ME and MAE respectively.

Applying the LSIC methods, the ME for the HOMO energy and total energy is seen to drop from more than 60% for both LSDA and PBE and thereby reducing the error. We notice that there is a sign change in the change in total energy, which is underestimated for LSDA and overestimated for PBE, and the reverse is the case for the change in HOMO energy computed.

The VDEs compute with LSIC PBE have the less error of 30.565 meV followed by LSIC LSDA with an error of 45.76meV and both LSDA and PBE are better when compare with MP2(46.18 meV). There is great improvement in the LSIC HOMO energy as it has twice the value FLOSIC PBE which have confirmed to have better estimate of the homo energy.

The VDE computed for branched octamer structure can be seen to have a linear trimer cluster having it end hydrogens bonded to dimer and trimer unlike the heptamer whose bounding form a loop. However, we find that the values of VDE strongly depend on the number linear chain bond in the configuration.

4.3: Conclusion.

We studied the vertical detachment energies VDEs of ammonia cluster anions using locally scaled SI-corrected DFAs. We show that the results obtained using LSIC for the VDE both using Total energy and negative of the HOMO energy. The most notable feature is that the LSIC correction leads to a substantial improvement over the FLOSIC and PZSIC in predicting the VDE.

The VDEs predicted by the LSIC method are in excellent agreement with the CCSD(T) values. The absolute HOMO energy of LSIC with LDA and FLOSIC with PBE functional provide excellent estimates of the electron removal energy for chain ammonia cluster anions.

The future work is using a different iso-orbital indicator and full variational LSIC implementation.

References

[1] W. R. Garrett, (1971). Phys. Rev. A 3, 961

[2] K. D. Jordan and F. Wang, (2003). Annual Review of Physical Chemistry 54,367.

and K. H. Bowen, (2004). The Journal of Chemical Physics 120, 685.

[3] N. I. Hammer, R. J. Hinde, R. N. Compton, K. Diri, K. D. Jordan, D. Radisic, S. T. Stokes, (2004). Journal of Chemical Physics 120, 685.

[4] J. P. Perdew and A. Zunger, (1981). Phys. Rev. B 23,5048.

[5] L. A. Cole and J. P. Perdew, (1982). Phys. Rev. A 525, 1265.

[6] Herbert, J,.M.;Head-Gordon, (2006). M.J.Phys.Chem. 8,68.

[7] F. Jensen, (2010). Journal of Chemical Theory and Computation 6, 2726 MID: 26616074.

[8] Y. Zhang, P. M. Weber, and H. Jnsson, (2016). The Journal of Physical Chemistry Letters 7, 2068.

[9] Kiyoshi Yagi, Yuko Okano, Takeshi Sato, Yukio Kawashima, Takao Tsuneda and Kimihiko Hirao (2008). J.Phys.Chem. A,112, 9845-9853.

[10] Richard M Martin. (2004). Electronic structure: basic theory and practical methods. Cambridge University Press, Cambridge.

[11] Walter Kohn, Axel D Becke, and Robert G Parr. (1996). Density functional theory of electronic structure. The Journal of Physical Chemistry, 100(31):12974–12980.

[12] Walter Kohn and Lu Jeu Sham. (1965). Self-consistent equations including exchange and correlation effects. Physical Review, 140(4A): A1133.

[13] Pierre Hohenberg and Walter Kohn. (1964). Inhomogeneous electron gas. Physical Review, 136(3B): B864,

[14] John P Perdew, Kieron Burke, and Matthias Ernzerhof. (1996). Generalized gradient

approximation made simple. Physical Review Letters, 77(18):3865.

[15] John P Perdew and Yue Wang. (1992). Accurate and simple analytic representation of the electron-gas correlation energy. Physical Review B, 45(23):13244.

[16] John P Perdew and Adrienn Ruzsinszky. (2010). Density functional theory of electronic structure: a short course for mineralogists and geophysicists. Reviews in Mineralogy and Geochemistry, 71(1):1–18.

[17] Takao Tsuneda. (2014). Density functional theory in quantum chemistry. Springer Science & Business Media, Tokyo.

[18] Aron J Cohen, Paula Mori-Sánchez, and Weitao Yang. (2011). Challenges for density functional theory. Chemical Reviews, 112(1):289–320.

[19] John P Perdew and Alex Zunger. (1981). Self-interaction correction to density-functional approximations for many-electron systems. Physical Review B, 23(10):5048.

[20] Mark R Pederson. (2015). Fermi orbital derivatives in self-interaction corrected density functional theory: applications to closed shell atoms. The Journal of Chemical Physics, 142(6):064112.

[21] Susanne Yelin, E Arimondo, and Chun Lin, editors. (2015). Advances in atomic, molecular, and optical physics, volume 64 of Advances in atomic, molecular, and optical physics. Academic Press, Amsterdam, 1. Edition.

[22] Mark R Pederson, Richard A Heaton, and Chun C Lin. (1984). Local-density Hartree-Fock theory of electronic states of molecules with self-interaction correction. The Journal of Chemical Physics, 80(5):1972–1975.

[23] Simon Klüpfel, Peter Klüpfel, and Hannes Jónsson. (2012). The effect of the Perdew-

Zunger self-interaction correction to density functionals on the energetics of small molecules. The Journal of Chemical Physics, 137(12):124102.

[24] Mark R Pederson, Richard A Heaton, and Chun C Lin. (1985). Density-functional theory with self-interaction correction: application to the lithium molecule. The Journal of Chemical Physics, 82(6):2688–2699.

[25] Mark R Pederson, Richard A Heaton, and Joseph G Harrison. (1989). Metallic state of the free-electron gas within the self-interaction-corrected local-spin-density approximation. Physical Review B, 39(3):1581.

[26] Takao Tsuneda and Kimihiko Hirao. (2014). Self-interaction corrections in density functional theory. The Journal of Chemical Physics, 140(18):18A513.

[27] Mark R Pederson, Tunna Baruah, Der-you Kao, and Luis Basurto. (2016). Self-interaction corrections applied to Mg-porphyrin, C60, and pentacene molecules. The Journal of Chemical Physics, 144(16):164117.

[28] Mark R Pederson, Adrienn Ruzsinszky, and John P Perdew. (2014). Self-interaction correction with unitary invariance in density functional theory.

[29] Zeng-hui Yang, Mark R Pederson, and John P Perdew. (2017). Full self-consistency in the Fermi-orbital self-interaction correction. Physical Review A, 95(5):052505.

[30] Torsten Hahn, Simon Liebing, Jens Kortus, and Mark R Pederson. (2015). Fermi orbital self-interaction corrected electronic structure of molecules beyond local density approximation. The Journal of Chemical physics, **143**(22):224104.

[31] J W Linnett. (1960). Valence-bond structures: a new proposal. Nature, 187(4740):859–861.

[32] J W Linnett. (1961). A modification of the Lewis-Langmuir octet rule. Journal of the American Chemical Society, 83(12):2643–2653.

[33] Gilbert N Lewis. (1916). The atom and the molecule. Journal of the American Chemical Society, 38(4):762–785.

[34] Walter Heitler and Fritz London. (1927). Interaction between neutral atoms and homopolar binding according to quantum mechanics. Zeitschrift für Physik, 44:455.

[35] Friedrich Hund. Zur Deutung der Molekel spektren. IV. (1928). Zeitschrift für Physik, 51(11):759–795.

[36] Robert S Mulliken. (1928). The assignment of quantum numbers for electrons in molecules. I. Physical Review, 32(2):**186.**

[37] Robert S Mulliken. (1928), The assignment of quantum numbers for electrons in molecules. II. Correlation of molecular and atomic electron states. Physical Review, 32(5):**761**.

[38] Mark R Pederson and Chun C Lin. (1988). Localized and canonical atomic orbitals in self-interaction corrected local density functional approximation. The Journal of Chemical Physics, 88(3):1807–1817.

[39] Jakob Kraus. (2017). A density functional study on neutral (Fe2O3)n clusters (n=1-3): comparing LDA and GGA approaches. Seminar Thesis, TU Bergakademie Freiberg, Freiberg.

[39] John P Perdew and Mel Levy. (2017). Physical content of the exact Kohn-Sham orbital energies: band gaps and derivative discontinuities. Physical Review Letters,

[40] M. R. Pederson and K. A. Jackson, (1990). Phys. Rev. B. 41, 7453.

[41] K. A. Jackson and M. R. Pederson, (1990). Phys. Rev. B. 42, 3276.

[42] M. R. Pederson and K. A. Jackson, (1991). Phys. Rev. B. 43, 7312.

[43] A. A. Quong, M. R. Pederson, and J. L. Feldman, (1993). Solid State Commun. 87, 535.

[44] D. V. Porezag and M. R. Pederson, (1996). Phys. Rev. B. 54, 7830.

[45] D. V. Porezag, (1997).. PhD thesis: http://archiv.tu-chemnitz.de/pub/1997/0025

[46] A. Briley, M. R. Pederson, K. A. Jackson, D. C. Patton, and D. V. Porezag, (1998). Phys. Rev. B. 58, 1786.

[47] Jianwei Sun,Adrienn Ruzsinszky and John P. Perdew (2015). Physicals review letters PRL 115, 036402

[48] H. Yu, S. Li, and D. Truhlar, (2016) The Journal of chemical physics 145 13, 130901.

[49] F. Malet and P. Gori-Giorgi, (2012) Physical review letters 109, 246402.

[50] R. O. Jones, (2015) Reviews of modern physics 87, 897.

[51] J. P. Perdew and A. Zunger, (1981) Phys. Rev. B23, 5048. URLhttps://link.aps.org/doi/10.1103/PhysRevB.23.5048.

[52] M. Levy, J. P. Perdew, and V. Sahni, (1984) Physical Review A30, 2745.

[53] J. P. Perdew and A. Zunger, (1981) Phys. Rev. B23, 5048,

[54] L. Yu and Z.-Z. Yang, (2010) The Journal of chemical physics 132, 174109.

[55] I. A. Shkrob, (2006) The Journal of Physical Chemistry A110, 3967.

[56] B. Baranyi and L. Turi, The Journal of chemical physics 151, 204304 (2019).

[57] Y. Yamamoto, C. M. Diaz, L. Basurto, K. A. Jackson, T. Baruah, and R. R. Zope, (2019) The Journal of Chemical Physics151,154105.

[58] R. R. Zope, Y. Yamamoto, C. M. Diaz, T. Baruah, J. E. Peralta, K. A. Jackson, B. Santra, and J. P. Perdew, (2019) The Journal of Chemical Physics151, 214108.

[59] J. Vargas, P. Ufondu, T. Baruah, Y. Yamamoto, K. A. Jackson, and R. R. Zope, (2020) Physical Chemistry Chemical Physics 22, 3789.

[60] http://jmol.sourceforge.net/.

[61] W. Weyl, ann.(1864) phys.Chem. 197,601.

[62] C.A. Kraus,(1908) J.Am. Chem.Soc. 30,1323

[63] W. L. Jolly, (1972)Metal-Ammonia Solutions (Dowden, Hutchinson, and Ross, Stroudsburg, PA.

[64] I. A. Shkrob,(2006) J. Phys. Chem. A 110, 3967.

[65] T. Sommerfeld, (2008) J. Phys. Chem. A 112, 11817.

Vita

Peter Obinna Ufondu was born in Lagos, Nigeria. He completed his Bachelor of Technology degree in Physics from the Federal University of Technology Owerri (FUTO), which is the top-ranked prestigious university of technology in Nigeria. He joined the University of Texas at El Paso in Spring, 2018 as a Physics certificate graduate student before switching to the physics master program in Fall, 2018. He got his Master of Science in Physics in August 2019.

He was admitted to the master's program in computational science in Fall 2019. During his studies at the University of Texas at El Paso UTEP, he got the opportunity to work as a Teaching Assistant and Research Assistant in both the Physics department and computational science program. His research is major in describing the characteristics of weakly bound cluster anion using self-interaction corrected density functional theory.

In Fall of 2021, he will be pursuing a doctorate degree in Physics from the University of Saskatchewan in Canada.

Permanent address: 5 Ifelodun street Egan, Igando Lagos State. Nigeria.
Email: peter.ufondu@ yahoo.com
This thesis was typed by Peter Obinna Ufondu